Article ID: 1006-8775(2016) 01-0030-12

MODULATION OF MADDEN-JULIAN OSCILLATION ON TIBETAN PLATEAU VORTEX

ZHAO Fu-hu (赵福虎)[1], LI Guo-ping (李国平)[2,3], HUANG Chu-hui (黄楚惠)[4], LIU Xiao-ran (刘晓冉)[5]
(1. Chongqing Meteorological Observatory, Chongqing 401147 China; 2. College of Atmospheric Sciences, Chengdu University of Information Technology, Chengdu 610225 China; 3. Collaborative Innovation Center on Forecast and Evaluation of Meteorological Disasters, Nanjing University of Information Science & Technology, Nanjing 210044 China; 4. Sichuan Meteorological Observatory, Chengdu 610072 China; 5. Chongqing Climate Center, Chongqing 401147 China)

Abstract: This study uses NCEP/NCAR daily reanalysis data, NOAA outgoing long-wave radiation (OLR) data, the real-time multivariate MJO (RMM) index from the Australian Bureau of Meteorology and Tibetan Plateau vortex (TPV) data from the Chengdu Institute of Plateau Meteorology to discuss modulation of the Madden-Julian Oscillation (MJO) on the Tibetan Plateau Vortex (TPV). Wavelet and composite analysis are used. Results show that the MJO plays an important role in the occurrence of the TPV that the number of TPVs generated within an active period of the MJO is three times as much as that during an inactive period. In addition, during the active period, the number of the TPVs generated in phases 1 and 2 is larger than that in phases 3 and 7. After compositing phases 1 and 7 separately, all meteorological elements in phase 1 are apparently conducive to the generation of the TPV, whereas those in phase 7 are somewhat constrained. With its eastward propagation process, the MJO convection centre spreads eastward, and the vertical circulation within the tropical atmosphere changes. Due to the interaction between the mid-latitude and low-latitude atmosphere, changes occur in the baroclinic characteristics of the atmosphere, the available potential energy and eddy available potential energy of the atmosphere, and the circulation structures of the atmosphere over the Tibetan Plateau (TP) and surrounding areas. This results in significantly different water vapour transportation and latent heat distribution. Advantageous and disadvantageous conditions therefore alternate, leading to a significant difference among the numbers of plateau vortex in different phases.

Key words: modulation; wavelet analysis; composite analysis; low-frequency oscillation; Tibetan Plateau vortex; real-time multivariate MJO index
CLC number: P434.4 **Document code:** A
doi: 10.16555/j.1006-8775.2016.01.004

1 INTRODUCTION

The Tibetan Plateau vortex (TPV) is a low vortex system situated at 500 hPa that is generated and developed on the main area of the Tibetan Plateau (TP). It usually disappears when it reaches the leeward eastern side of the TP and rarely moves out of the main area of the TP. However, under certain types of atmospheric circulation, it moves eastwards out of the TP and causes flooding in downstream areas (Yu and Gao[1]).

Pioneering research on the TPV initially focused on its formation mechanism [2], and the Lhasa Group of Tibetan Plateau Meteorology Research conducted substantial research in this respect[3]. Over the past 20 years, researchers have studied the TPV from different perspectives. For example, Yang and Luo[4] determined that vertical transportation of cumulus convection is considerably important in relation to the occurrence and development of the TPV and that the disturbance kinetic energy of the TPV is related to the convergence of disturbance kinetic energy and disturbance available potential energy. In addition, Luo et al.[5] concluded that the vertical transportation of water vapour and surface sensible heat causes a reduced depth of the western TPV under the cumulus and convection influence, which is beneficial for the generation and eastward movement of the warm TPV. Using numerical experiments, Ding et al.[6] revealed that the shear line and special underlying surface of the TP provide dynamic and thermodynamic conditions for the TPV, respectively. Furthermore, Chen et al.[7] found that the TPV is generated under a condition of strong surface heating, strong unstable stratification and condensation latent heat over the TP. Among them, surface sensible heat plays an important role in the formation of the TPV, and latent heat rising in a column from the ground has an important influence on the eastward movement and development of the TPV.

Yu and He [8] concluded that water vapour supply

Received 2014-05-16; **Revised** 2015-09-29; **Accepted** 2016-01-15
Foundation item: National Basic Research Program of China (2012CB417202); National Natural Science Foundation of China (41175045, 91337215, U1133603); Special Fund for Meteorological Research in the Public Interest (GYHY201206042)
Biography: ZHAO Fu-hu, M.S., primarily undertaking research on plateau meteorology and weather dynamics.
Corresponding author: LI Guo-ping, e-mail: liguoping@cuit.edu.cn

plays an important role in the generation and development of the TPV and that the water vapour in the higher troposphere over the TP is mainly from the Arabian Sea and the Indian Ocean. They also pointed out that the enhancement of water vapour transportation in the southern TP causes the 500-hPa geopotential height contour line a cyclonic curve, which is therefore extremely relevant to the occurrence of the TPV.

Other studies, such as that of Li et al.[9], used dynamic analysis to confirm that surface sensible heat, heat force, and the action of dynamic pumping in the boundary layer play an important role in the generation and development of the TPV(Li and Xu[10]; Li and Liu[11]). Gao and Ping [12] found that the shedding vortex in the leeward district of the eastern side of the TP, propagates downstream in the form of wave propagation. Yu et al. [13, 14] demonstrated that cold air flow has a strong influence on the occurrence of the TPV and that the convergence of dry cold air and moist warm air enhances the baroclinic instability of the atmosphere and contributes to the development and eastward movement of the TPV. Furthermore, He et al.[15] then confirmed that the prevalent northern airflow near or north of the TPV area and the leeward slope behind the large terrain are more likely to lead to the development of TPV. They also concluded that the southward movement of cold air triggering the release of atmospheric unstable energy is an important mechanism in the development of the TPV, while the convergence of warm and cool air over the TP grealty influences the maintenance and development of the TPV. In addition, they proved that the TPV easily occurs over high altitude terrain and steep slope regions and that the TP heating and the dynamic and thermodynamic functions of steep terrain cause its formation (He et al.[15, 16]). Liu and Li[17] solved the KdV equation to reveal that the TPV is similar to a tropical cyclone and that it also has a warm core, which is not only the result of the TP adiabatic heating but also the need for vortex motion to maintain the gradient wind balance and static balance. Chen and Li [18] demonstrated that the thermal effect and the boundary layer effect of the TP play an important role in the circulation structure of the TPV, and Song et al [19]. used numerical experiments to determine that thermal conditions have a significant influence on the formation, development and structural change of the TPV.

In the early 1970s, Madden and Julian discovered the existence of an atmospheric low-frequency oscillation occurring in tropical regions, which was subsequently named the Madden-Julian oscillation (MJO) (Madden and Julian[20, 21]). Krishnamurti then determined the MJO to be a widespread phenomenon in the atmosphere (Krishnamurti and Gadgil[22]). Recently, scientists have conducted considerable research on the MJO, such as its effect on the monsoon (Yasunari[23]; Zhu[24]; Miao and Liu[25]; Jun and Sun[26]; Li and Wu[27]; Ju et al.[28]; Ju and Zhao [29]), weather, climate (Chen et al.[30]; Lu and Ding [31]; Huand and Zhu [32]; Chen et al.[33]; Xu et al.[34]; Zhou et al.[35]; Lu et al.[36]; He et al.[37]), ENSO and many other aspects (Li and Zhou[38]; Li and Liao[39]; Long and Li[40]; Qiu et al.[41, 42]).

Although a number of studies have been conducted on the MJO in relation to the TP (Sun and Chen[43]; Xie et al.[44]; Li [45]; Gong et al.[46]; Peng et al.[47]), research directly associated with the TPV is limited, and previous studies have mainly focused on the relationship between the clustering of the TPV and the MJO (Zhang et al.[48]; Sun and Chen [49]; Zhang et al.[50]). It is acknowledged that the TPV has a relatively similar structure to a typhoon in some respects [1-17], and the influence of the MJO on Western Pacific typhoons has been well studied (Pan et al.[51]; Li et al.[52]). However, studies on the relationship between the MJO and the TPV are rare, and therefore, we focus on this relationship in our study.

2 DATA AND METHODS

The data used in this paper are as follows: reanalysis data (zonal wind, meridional wind, geopotential height, air temperature and atmospheric humidity) with a spatial resolution of 2.5°×2.5°, obtained from the National Center for Environmental Prediction/National Center for Atmospheric Research (NCEP/NCAR); daily satellite-observed outgoing long-wave radiation (OLR) data with a spatial resolution of 2.5°×2.5° from the National Oceanic and Atmospheric Administration (NOAA); the real-time multivariate MJO (RMM) index from the Australian Bureau of Meteorology and statistical TPV data from the Chengdu Institute of Plateau Meteorology of CMA. The RMM index was first created and used by Wheeler and Hendon [53] as well as Peng et al.[47], and was then used worldwide (for example, by the Australian Bureau of Meteorology, the U.S. Climate Prediction Center (CPC) and the Japan Meteorological Agency). It is considered to be an effective tool for use in short-term climate prediction as it is able to reveal the amplitude (intensity) and the propagation process (convection position) of the MJO.

Combination fields of near-equatorially averaged 850-hPa zonal wind, 200-hPa zonal wind and satellite-observed OLR data (each averaged over the latitudes at 15° S –15° N) are chosen for EOF analysis, where daily observed data were projected on to the multiple-variable EOFs. The resulting pairs of time series from the desired index are referred to as the real-time multivariate MJO series 1 (RMM1) and 2 (RMM2). These vary mostly on the intraseasonal time scale of the MJO only, with an amplitude of $\sqrt{RMM1^2+RMM2^2}$.

The statistical method employed in the study of the TPV uses the real-time multivariate MJO index (RMM) to examine the strength of the MJO. Two different metrics are determined using amplitudes 1 and 0.8 (where a value greater than 1 (0.8) corresponds with active MJO periods, and a value of less than 1 (0.8) corresponds to

suppressed MJO periods). In this paper, we count the frequency of the TPV in active and suppressed periods of the MJO respectively, in addition to the frequency distribution in different phases of active MJO periods.

In this study, wavelet analysis is also used to determine the atmospheric oscillation cycle of the various meteorological elements in the TP, and the Lanczos band-pass filter is then used for oscillation cycle filtering. The TP region is defined as being mainly in the range of 27.5–40°N, 75–105°E.

3 ANALYSIS OF ATMOSPHERIC OSCILLATION CYCLE OVER TP AND STATISTICAL CHARACTERISTICS OF TPV

3.1 *Analysis of atmospheric oscillation cycle over TP*

Wavelet analysis was used to determine the low-frequency oscillation cycles of meteorological elements recorded between 1998 and 2010 over the TP. Results showed that each element had oscillation characteristics of a 30- to 60-day cycle. Further investigations showed an oscillation cycle of 30- to 60-day to be particularly significant in the following fields: the 200-hPa zonal wind field, 500-hPa wind zonal field, OLR field and the 500-hPa geopotential height field (Fig.1).

As can be seen in the wavelet power spectrum shown on the left of Fig.1a, the oscillation cycle of 30–60 day is quite strong in winter and spring, but relatively weak in autumn and summer. To verify that this phenomenon is not only a unique characteristic of the 200-hPa zonal wind field, we examined the 500-hPa zonal wind field, OLR field and 500-hPa geopotential height field and found the existence of this phenomenon in these fields (Fig.1b, 1c and 1d). We then used a Lanczos band-pass filter to extract the low-frequency component of 30–60 day that could have an effect on the TPV).

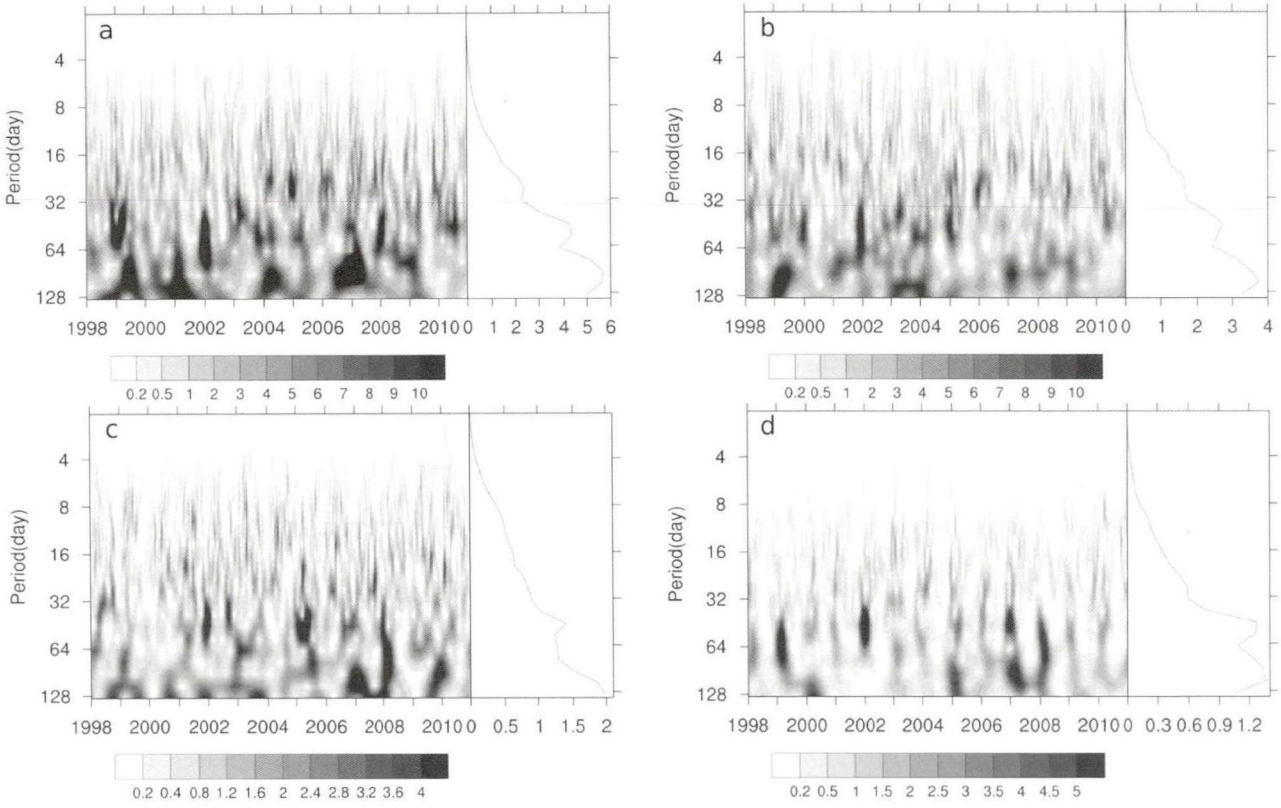

Figure 1. Analysis of wavelet power spectrum (left) and variance (right) of daily standardized series of each regional average variable over the TP from 1998 to 2010. (a) 200-hPa u wind field; (b) 500-hPa u wind field; (c) OLR field; (d) 500-hPa geopotential height field (Morlet wavelet is used and shadings indicate the 95% confidence level).

3.2 *Distribution of TPV in different MJO phases*

Under both MJO measurement standards, Table 1 shows statistical results of the TPV frequency distribution in each phase of the active MJO periods during onset and duration, and the TPV frequency differences between the active and suppressed periods of the MJO. As can be seen from the above statistics, there is a far greater frequency of the TPV in the active phase of the MJO than in the suppressed phase, and this indicates that the occurrence of the TPV is more likely during a strong MJO process.

On examining the TPV frequency distribution in each active MJO phase during the onset period, under both MJO measurement standards, it can be seen that

Table 1. Statistical results of TPV frequency in different phases of MJO.

	MJO amplitude	TPV frequency in different phases of the MJO								active /suppressed amplitude=1.0	active /suppressed amplitude=0.8
		phase1	phase2	phase3	phase4	phase5	phase6	phase7	phase8		
Onset	>0	99	82	48	54	61	57	41	67	314:193	381:126
	>1.0	71	49	25	32	34	31	27	46		
	>0.8	84	63	31	40	40	40	33	51		
duration	>0	154	143	73	86	79	86	80	94	491:301	588:204
	>1.0	104	89	43	51	46	55	44	60		
	>0.8	126	109	50	63	50	64	61	70		

there is a significant increase (above normal) in TPV frequency in phase 1 and 2, while there is a significantly reduced frequency (below normal) in phase 3 and 7. In addition, examination of the TPV frequency distribution in each active MJO phase throughout the duration period shows that there is also a significantly increased frequency (above normal) in phase 1 and 2. It should be noted that different standard measurements used for the MJO correspond to different lower frequency phases of the MJO. The standard measurement of amplitude 1 corresponds to phase 3 and 5, and amplitude 0.8 corresponds to phase 3 and 7. The above differences are due to differing statistical standards and unobvious distinctions among the TPV frequency distribution in the low frequency phase. However, these conclusions are significantly different from study of Li and Pan for the Western Pacific typhoon; they found that the typhoon generation frequency in phase 2 and 3 is significantly less than normal and that in phase 5 and 6 is more obvious.

As can be seen from the above analysis, the modulation mechanism of the MJO on the TPV is significantly different from that on the Western Pacific typhoon. The modulation effect of the MJO on the TPV is significant, and the TPV frequencies in the onset and duration periods change with the eastward movement of the MJO (strong convection centre and eastward movement of the MJO.

To explore reasons for the high frequency and low frequency phase-locked phenomenon of the TPV and to investigate the role of the MJO modulation on the TPV, we respectively synthesized phase 1 as its highest TPV frequency and phase 7 with a relatively low TPV frequency. We did not choose phase 3 with the lowest TPV frequency, because the suppression factor of the TPV in this phase is not obvious. The following synthesis analysis is conducted in accordance with current practice at home and abroad, taking amplitude 1 as a measurement of MJO strength.

4 ANALYSIS OF DYNAMIC CONDITIONS INVOLVED IN TPV GENERATION DURING DIFFERENT PHASES

There are 394 days when the MJO is active in phase 1 during the study period (from 1998 to 2010), and the MJO convection centre is located in the tropical regions of North Africa, corresponding to a high TPV frequency. However, 320 days are represented by phase 7 of the active MJO period, and the MJO convection centre is located in the tropical regions of the Western Pacific, corresponding to a low TPV frequency. To determine reasons for the TPV frequency distribution differences between phase 1 and 7, we composited the low-frequency atmospheric circulation of two phases separately to examine the dynamic conditions of the MJO's effect on the generation of the TPV. Fig.2 shows a composite field of the low-frequency atmospheric circulation in the first phase (Figs. 2a and 2c) and the seventh phase (Figs.2b and 2d), at 500 hPa (Figs.2a and 2b) and 200 hPa (Figs.2c and 2d), respectively.

In the low-frequency atmospheric circulation composite field at 500 hPa in the first phase, the northeast airflow controls most of the plateau region. A low-pressure cyclone system with low-frequency lies over the Southern Highlands; the existence of this system causes the TPV frequency distribution in the first phase to be significantly above normal. However, in the seventh phase composite field, the TP is between two high-pressure anticyclone systems with low frequency, which is not conducive to the occurrence of the TPV. In the first phase, the low-frequency Western Pacific subtropical high extends westward to the east of the Indochina region. The Bay of Bengal, India and the Arabian Peninsula are controlled by a high-pressure anticyclone system with low-frequency, and the centre is over the Indian subcontinent. There are two southerly flows on the east and west sides of the high-pressure; one moves northward through the Indochina Peninsula and then along the trailing edge of the subtropical high, and the other moves northward through the east of the North African waters regions. In contrast, in the seventh phase, the Western Pacific and the Bay of Bengal are controlled by a low-pressure cyclone system with low-frequency, which hinders the transportation of water vapour from the Indian Ocean to the east of the TP.

In the first phase, Southwest China is in the control of a low-pressure cyclone system with low-frequency, and Eastern China is in the control of a high-pressure anticyclone system. The direction of water vapour transportation along the edge of the subtropical high system

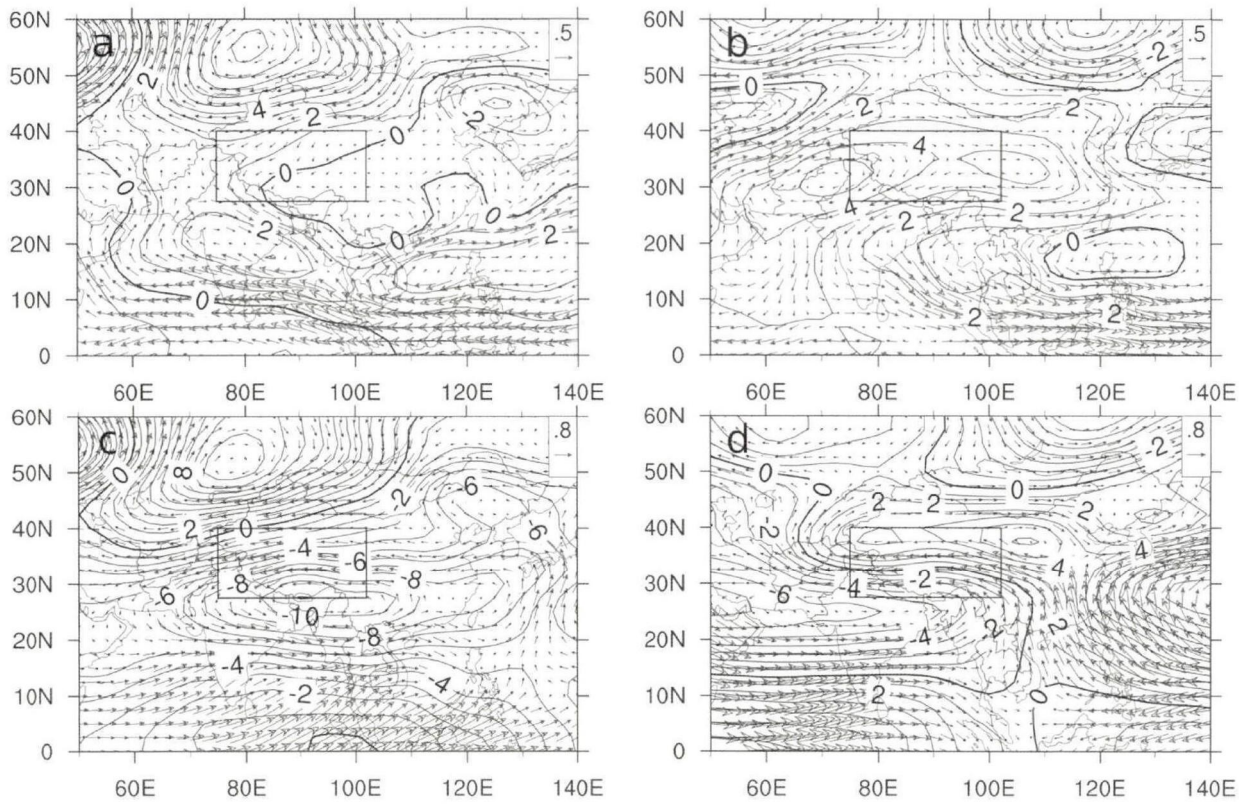

Figure 2. Atmospheric circulation composite fields with 30-60 day filtering in the (a, c) first and (b, d) seventh phases. Low-frequency wind field and low-frequency geopotential height field at (a, b) 500 hPa and (c, d) at 200 hPa. Unit: m/s, dagpm.

changes due to the existence of these two systems and causes the water vapour to be continuously transferred to the eastern plateau. The area in the north of Balkhash Lake is controlled by a powerful low-frequency blocking high, and Northeast China is in the control of a powerful low-pressure cyclone with low-frequency. However, in the seventh phase, the eastern part of China is situated at the front of a low frequency high-pressure anticyclone system with northerly airflow, thus it is difficult for water vapour to be transferred from the West Pacific to the eastern part of China and the eastern TP. The west of the Aral Sea is controlled by a low-frequency low pressure cyclone system, and the northeastern region of Balkhash Lake is controlled by a low-frequency cyclone system.

When the atmospheric circulation system configuration in the first phase is contrasted with that of the seventh phase, it can be seen that the configuration of 'high-low-high' from the equator to the mid-latitude in the first phase represents strong baroclinicity, high available atmospheric and vortex potential energy, and therefore it is evident that these conditions are required for the TPV in the first phase. An atmospheric configuration with a strong baroclinicity, high available atmospheric vortex potential energy are advantageous to the development of the TPV, and this conclusion is similar to that made by Yu et al.[13, 14].

For the composited low-frequency atmospheric circulation field of the first phase at 200 hPa (Fig.2c), the north of Balkhash Lake is in the control of a powerful low-frequency high pressure anticyclone, and the south of the TP is in the control of a strong low-frequency low pressure cyclone system. TP is situated between the two systems, and the main area of the TP is controlled by a strong easterly airflow, which is beneficial to the divergence of the upper troposphere and forms a 'pumping' effect that promotes the occurrence and development of the TPV. This verifies the concept that dynamic pumping has an important influence on the generation and development of the TPV, as proposed by Li and Liu [11]. The air over the southern plateau (from bottom to top) is under the control of a deep low-pressure cyclone system sloped to the south, which favors a high frequency TPV in the first phase. However, in phase 7, the air on the TP (from bottom to top) is under the control of a deep low-frequency high pressure anticyclonic system, which it is not conducive to the occurrence of the TPV.

A low-frequency vorticity difference can be seen between the first and seventh phases at 500 hPa and 200 hPa separately (Fig.3). As can be seen from the low-frequency vorticity difference field in Fig.3a at 500 hPa, there is a positive value over the TP, which reflects that convergence with an ascending motion in the

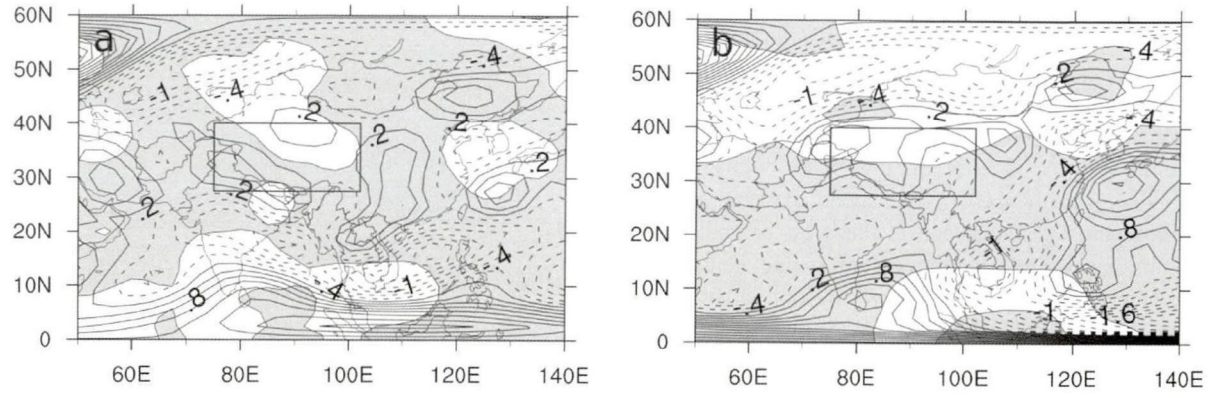

Figure 3. Difference fields of the low-frequency vorticity anomaly with 30–60 day filtering at (a) 500 hPa and (b) at 200 hPa. Unit: $10^{-5}\cdot s^{-1}$, shadows pass test at 0.1 significance levels.

first phase is stronger than that in the seventh phase over the TP; therefore, the first phase provides good dynamic conditions for the generation of the TPV. Fig.3b shows the low-frequency vorticity difference field at 200 hPa, which has negative areas in the eastern TP and positive areas in the western TP. This shows that high atmospheric convergence in the eastern TP is more significant in the first phase than in the seventh phase. The vorticity field collocation from low-level to high-level in the first phase is conductive to the occurrence of the TPV, yet it is not favourable to the occurrence of the TPV in the seventh phase.

Figure 4 shows the composite fields of low-frequency atmospheric vertical speed in the first phase (Figs. 4a and 4c) and seventh phase (Figs. 4b and 4d) at 500 hPa (Figs. 4a and 4b) and 700 hPa (Figs. 4c and 4d), respectively. As can be seen from Fig.4, in the first phase, the atmosphere vertical velocity field at 500 hPa in the eastern plateau presents a significant upward movement, with rising velocity high value centre in its southern part. Central Asia, together with central and eastern China are both controlled by updrafts, and rising

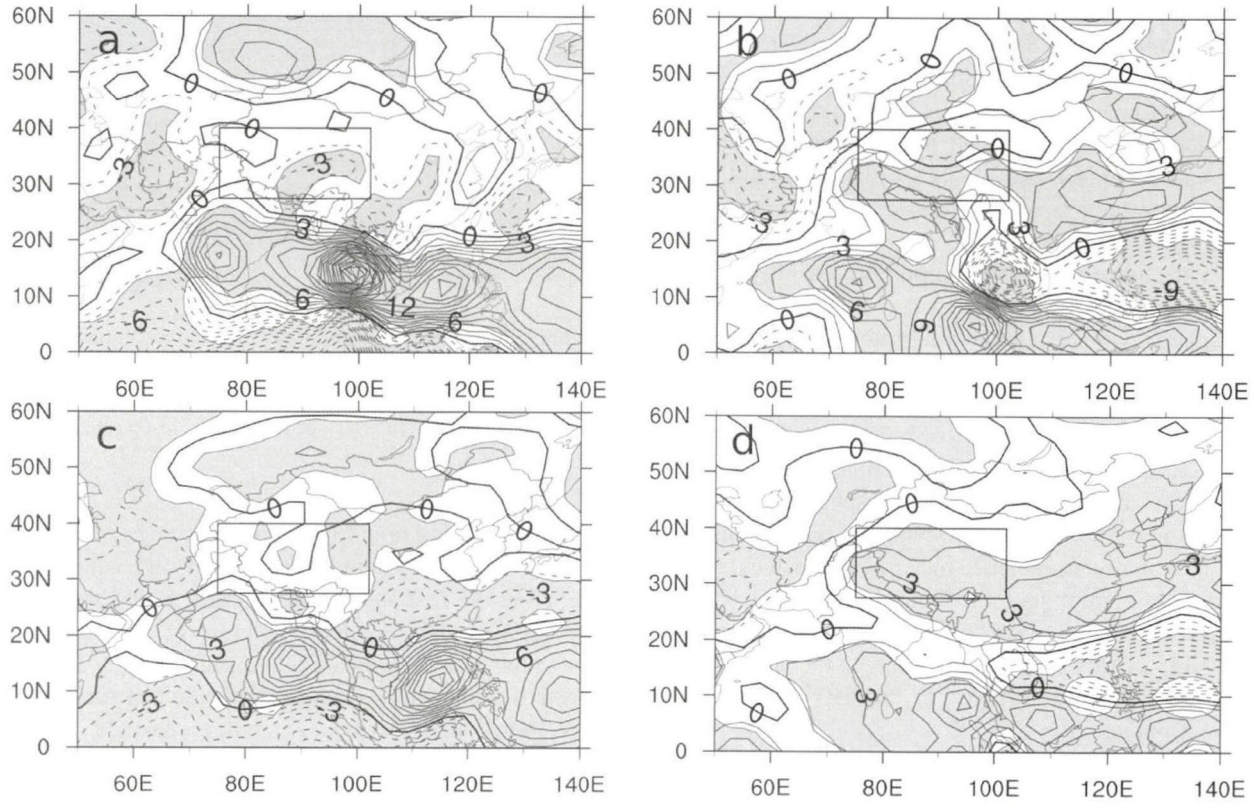

Figure 4. Vertical speed composite fields with 30–60 day filtering in (a, c) the first phase, (b, d) in the seventh phase at (a, b) 500 hPa and (c, d) at 200 hPa. Unit: $Pa\cdot s^{-1}$, shadows pass test at 0.1 significance levels.

velocity high value centers are located in the east of the Iranian Plateau and the eastern part of China. The upward movement in the equatorial region is also quite obvious. In contrast, the high latitudes and the large area from the Western Pacific to the Arabian Sea are well controlled by sinking airflow, and over the Indochina Peninsula is the sinking speed extreme center. In addition, the Western Pacific, the west of India and the South China Sea also have high value centres of sinking speed respectively, but these are not as strong as that over the Indochina Peninsula. At 200 hPa, the eastern plateau is still controlled by rising airflow, yet the western plateau is controlled by sinking airflow. The distribution situations of other parts are similar to those at 500 hPa, but the distribution of the centre is slightly different.

In the composite field of the seventh phase at 500 hPa, most areas of the TP are controlled by sinking airflow, and only the northern plateau is controlled by rising airflow. In addition, the northern and eastern parts of China and the tropic regions from the Western Pacific to the Indian Ocean are controlled by sinking airflow, while central Asia and subtropical regions of the Western Pacific are controlled by rising airflow. At 200 hPa, there is a sinking airflow area over the TP, with sinking speed high value centre over the southwestern plateau, but the distribution over other parts is similar to that at 500 hPa.

In summary, in the first phase the convection centre of the MJO is located in tropical regions in North Africa, and the TP is mainly controlled by updraft, which provides good conditions for the generation of the TPV. However, in the seventh phase, the convection centre of the MJO is located in the tropical regions of the Western Pacific, and the TP is mainly controlled by downdraft, which is not conducive to the formation of the TPV.

With the eastward propagation process of the MJO, the convection centre moves to the east and the tropical atmospheric vertical circulation structure changes. Due to the interaction between the atmospheric circulation at lower and middle latitudes, the distribution of atmospheric baroclinicity, the atmospheric available potential energy and the eddy available potential energy change, making an alteration in the atmospheric circulation structure over the TP and surrounding areas. A discrepancy thus exists in the moisture transfer, which results in a different latent heat distribution over the plateau. In this respect there are alternating favourable and unfavourable factors for the generation of the TPV, resulting in significant differences of the TPV frequency in different phases.

We use the zonal wind difference between 100 hPa and 500 hPa to represent the vertical wind shear, and then composite the vertical wind shear in the first and seventh phases, respectively (Figs.5a and 5b). The distributions of both phases are similar, and both show a

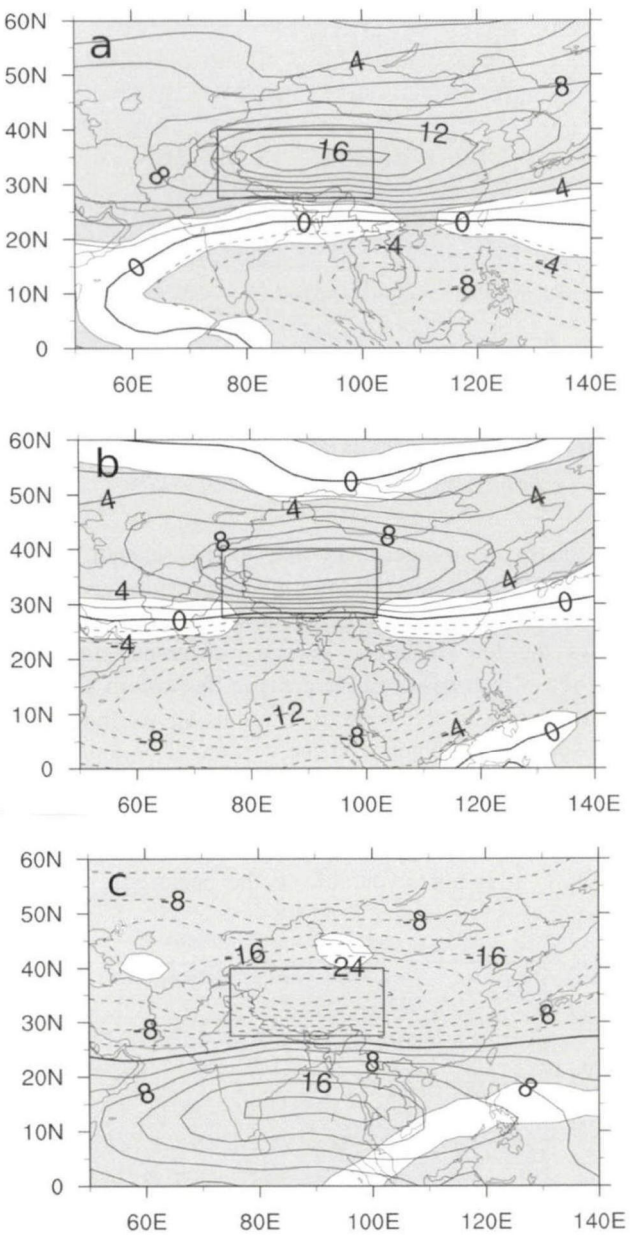

Figure 5. Vertical wind shear ($u_{100\text{-hPa}}$-$u_{500\text{-hPa}}$) composite fields in (a) the first phase; (b) the seventh phase and (c) difference fields of vertical wind shear between the first and seventh phases. Unit: $m.s^{-1}$, shadows pass test at 0.1 significance levels.

positive distribution in the north and a negative distribution in the south. There are closed positive centres over the TP in the first and seventh phases, which shows that the west wind is greater at high-level and smaller at low-level over the TP. Negative regions exist from the Western Pacific to the north of the Indian Ocean, and this shows that there is a stronger easterly wind at high-level and weaker easterly wind at low layers. The vertical wind shear between the upper and lower levels is strong over the TP, and it is therefore difficult for water vapour and heat to gather and a convection column to form; therefore it is not conducive for the for-

mation of the TPV.

In order to verify the above results, we analysed the difference between the first and seventh phases. Fig. 5c shows that there are negative values over the plateau regions, indicating that the vertical wind shear in the high-frequency phase is weaker than that in low-frequency phase. This indicates that the weaker vertical wind shear is advantageous to the generation of the TPV, while the stronger vertical shear is not. This result matches the result of Qian et al.[54].

5 ENERGY FIELD ANALYSIS FOR THE TPV IN DIFFERENT MJO PHASES

To compare the difference between convective activities in the first and seventh phases, we conducted an OLR difference between them (Fig.6). The values are negative in the southeastern TP, central and eastern China and northern Indian Ocean, which suggests in phase 1, that these regions have stronger convective activities and that the stronger convective activities over the southeastern TP are extremely conducive to the development of convective systems over the TP and the generation of the TPV. There is a positive banding zone from the Western Pacific to the Arabian Sea, with positive value centers in the east of the Philippines, South China Sea, the Bay of Bengal and the north of Arabian Sea respectively, and positive value exists in the middle and high latitudes as well. This indicates that convective activities over these regions are relatively weaker in the first phase compared to that in the seventh phase.

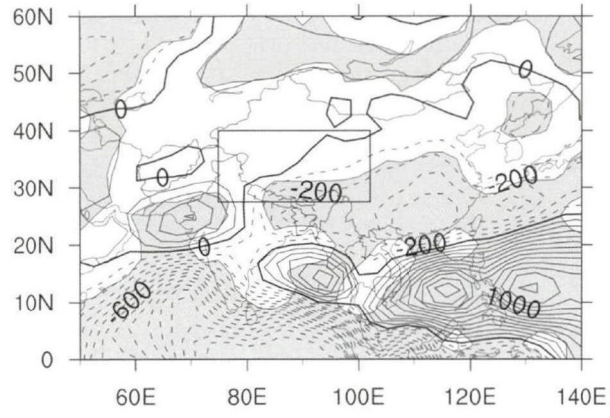

Figure 6. Difference field of OLR anomaly (with 30–60 day filtering) between the first and seventh phases. Unit: $W.m^{-2}$, shadows pass test at 0.1 significance levels.

Figure 7 shows the difference in low-frequency atmospheric kinetic energy between the first and seventh phases. This figure shows that within the scope of the TP the low-frequency kinetic energy in the first phase is lower than that in the seventh phase. Due to the energy conversion between kinetic and available potential energy, the atmospheric available potential energy is higher in the first phase, corresponding to a higher eddy available potential energy which is then conducive to the generation of a vortex system. Therefore, the lower the low-frequency energy distribution over the TP, the more conducive it is to the formation of the TPV.

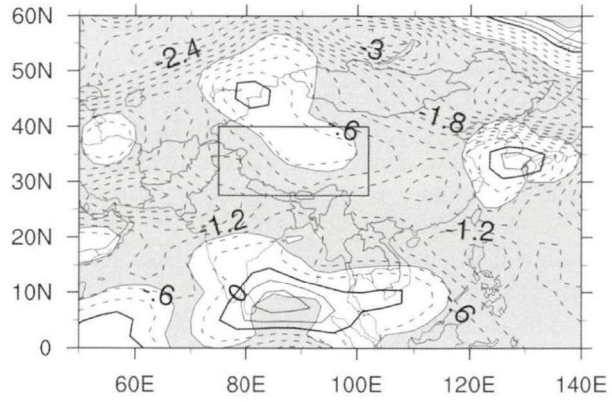

Figure 7. Difference field of kinetic energy anomaly (with 30-60 day filtering) between the first and seventh phases. Unit: $m^2.s^{-2}$, shadows pass test at 0.1 significance levels.

Figure 8 shows the temperature anomaly difference in TPV between the high frequency and the low frequency phases at different levels. In comparison with the seventh phase (Fig.8a), the temperature in the first

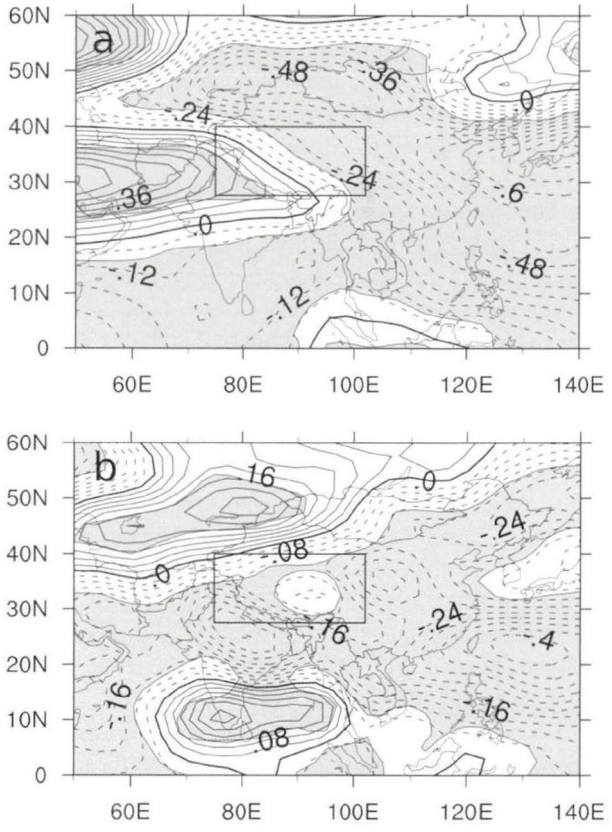

Figure 8. Difference field of temperature anomaly (with 30-60 day filtering) between the first and seventh phases at (a) 200 hPa and (b) 600 hPa (b). Unit: $m^2 \cdot s^{-2}$, shadows pass test at 0.1 significance levels.

phase at 200 hPa in the western TP is higher, while that in the eastern TP is lower, which shows there are more significant differences in the high-level temperature advection between the eastern and western TP. It also shows that cold advection at high-level is stronger in the eastern TP and warm advection at high-level is stronger in the western TP. Again, in comparison with the seventh phase, at 600 hPa (Fig.8b), temperatures are lower throughout the TP. This corresponds to stronger cold advection at low levels, and the distribution of atmospheric temperature is slightly different from the western side to the eastern side of the TP. It is considered therefore that temperature advection at low levels may be affected by the large terrain.

The quasi-barotropic state, generated by stronger cold advection at both high and low levels on the eastern side of the TP, is conducive for stimulating the formation of the TPV and to promoting the development of the TPV in the first phase.

6 DIFFERENCES IN MOISTURE CONDITIONS FOR THE GENERATION OF TPV IN DIFFERENT MJO PHASES

At the Lanzhou Institute of Plateau Atmospheric Physics, Chinese Academy of Sciences [2] it was pointed out that the prevailing southerly airflow on the eastern side of the TP makes the warm and moist air gathering there, with a large amount of latent heat, thereby creating conditions for the formation and development of the TPV. The moisture condition has an important role in the formation and development of the TPV, and therefore, we investigated the differences in the water vapour between the first and seventh phases.

The water vapour flux vector and water vapour flux divergence (Fig.9) in both phases suggest that the water vapour is transported continuously to the TP from the Arabian Sea and the Indian Ocean, with divergence of the water vapour in the western highlands over TP and convergence in the eastern highlands. To compare the difference between the TPV high frequency phase and the TPV low frequency phase, we show the difference between the first and seventh phases in Fig.7. The results show that water vapour transportation is stronger from the Arabian Sea and the Indian Ocean to the eastern TP in the first phase, and moisture convergence is more significant in the eastern TP. This was also clarified in the difference fields of atmospheric specific humidity in Fig.10; the first phase shows an evident 'dry in the east and wet in the west' distribution over the TP. This means that there is a more intense moisture divergence in the western highland region, and a more intense moisture convergence in the eastern region in the first phase; this distribution of water vapour is favourable for the formation of the eastern TPV.

Water vapour provides latent heat for the TPV and is an important source of energy for its development. Differences in the moisture condition in various phases results in a significantly different TPV frequency distribution; therefore, water vapour is very important factor in the generation of the TPV.

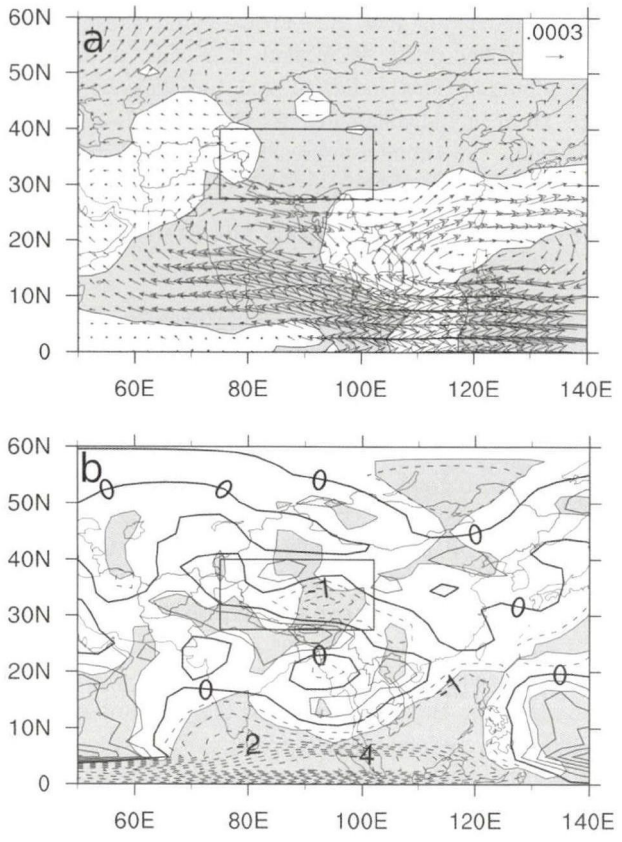

Figure 9. Difference field of water vapour anomaly (with 30-60 day filtering) between the first and seventh phases at 600 hPa; (a) water vapour flux (unit: $kg.m^{-1}.s^{-1}$); (b) water vapour flux divergence (unit: $kg.m^{-1}.s^{-1}$). Shadows pass test at 0.1 significance levels.

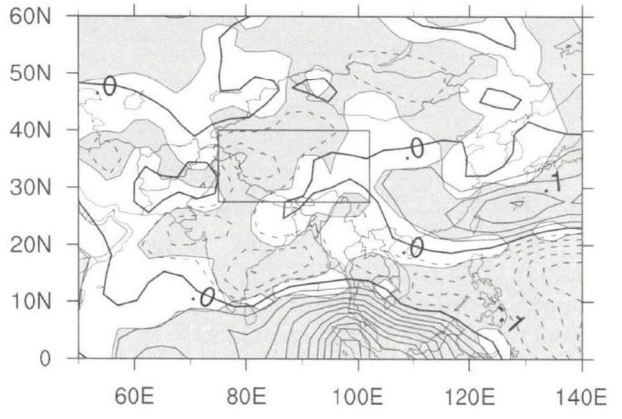

Figure 10. Difference field of atmospheric specific humidity (with 30-60 day filtering) between first and seventh phases at 600 hPa. Unit: $g.kg^{-1}$, shadows pass test at 0.1 significance levels.

7 CONCLUSIONS AND DISCUSSION

(1) The TPV is mainly generated in the active phase of the MJO; the TPV occurred 381 times in the

active phase and 126 times in the suppressed MJO phase between 1998 and 2010 (ratio of frequency of about 3:1). In the active phase of the MJO, the number of TPVs generated in the first and second phases is greater than that in the third and seventh phases, which shows that the MJO has a significant role in modulating the generation of the TPV.

(2) Within the scope of the TP, the cycle oscillation of 30 to 60 day is significant, and a strong feature is apparent in winter and spring and a weak feature in summer and autumn.

(3) The first phase (the high frequency phase of the TPV) presents a variety of beneficial conditions for TPV formation, such as the presence of a low-frequency low-pressure cyclonic circulation over the TP, larger low-frequency positive vorticity, faster low-frequency velocity, stronger moisture convergence, more intense convective activity, higher atmospheric available potential energy and eddy available potential energy. However, there are few beneficial factors in the seventh phase (low frequency phase of the TPV).

(4) A dynamic effect, good energy conditions and moisture transfers are the three main factors involved in the generation of the TPV.

(5) In the process of its eastward propagation, the convection centre of the MJO moves east. This corresponds to a change in the vertical structure of the atmospheric circulation in the tropics. Due to the interaction between the atmospheric circulation of the low and middle latitude regions, the distribution of atmospheric baroclinicity, atmospheric available potential energy and eddy available potential energy over these regions also changes, thereby changing the structure of atmospheric circulation over the TP and the surroundings. This makes a significant differentt water vapour transportation, which corresponds to the change in latent heat distribution, and provides advantageous and disadvantageous conditions for the TPV generation to appear alternately. This results in significant differences in the TPV frequency between different phases.

Statistical analysis preliminarily revealed the impact of the MJO on the TPV from different angles. However, for questions such as, 'Why are there differences in TPV frequency in strong and weak MJO phases?' and 'How do the physical mechanisms and pathways of the MJO influencing the TPV? ', it is also necessary to conduct further study based on numerical simulation and dynamic analysis. In addition, we need to know whether the MJO affects the TPV on its moving out of the TP, and how if there were effects? Such questions will be explored and answered in future work.

REFERENCES:

[1] YE Du-zheng, GAO You-xi. Meteorology of the Qinghai-Xizang Plateau [M]. Beijing: Science Press, 1979: 122-126 (in Chinese).

[2] Lanzhou Institute of Plateau Atmospheric, Physics of Chinese Academy of Sciences. Dynamic analysis of formation mechanism of the vortex on the eastern side of the Tibetan Plateau [J]. J Meteorol Sci Technol, 1977, 67(4): 54-65 (in Chinese).

[3] Lhasa Group of Tibetan Plateau Meteorology Research. The research on the development of the Tibetan Plateau vortex in midsummer [J]. Sci China, 1978, 8(3): 341-350 (in Chinese).

[4] YANG Yang, LUO Si-wei. Energy analyses of vortices over the Qinghai-Xizang Plateau in summer [J]. Quart J Appl Meteorol, 1992, 3(2): 199-205 (in Chinese).

[5] LUO Si-wei, HE Mei-lan, LIU Xiao-dong. Research on the Tibetan Plateau vortex [J]. Sci China (Ser B), 1993, 23(7): 778-784 (in Chinese).

[6] DING Zhi-ying, LIU Jing-Lei, LU Jun-ning. The study of the mechanism of forming Qinghai-Xizang vortex on 600 hPa [J]. Plateau Meteorol, 1994, 13(4): 411-418 (in Chinese).

[7] CHEN Bo-min, QIAN Zheng-an, ZHANG Li-sheng. Numerical Simulation of the formation and development of vortices over the Qinghai-Xizang Plateau in summer [J]. Chin J Atmos Sci, 1996, 20(4): 491-502 (in Chinese).

[8] YU Shu-hua, HE Guang-bi. Numerical experiment of influence of water vapor in the middle and upper troposphere on the formation of vortex over the Tibetan Plateau [J]. J Nanjing Inst Meteorol, 2001, 24(4): 553-559 (in Chinese).

[9] LI Guo-ping, ZHAO Bang-jie, YANG Jin-qing. A dynamical study of the role of surface sensible heating in the structure and intensification of the Tibetan Plateau vortices [J]. Chin J Atmos Sci, 2002, 26(4): 519-525 (in Chinese).

[10] LI Guo-Ping, XU Qi. Effect of dynamic pumping in the boundary layer on the Tibetan Plateau vortices [J]. Chin J Atmos Sci, 2005, 29(6): 965-972 (in Chinese).

[11] LI Guo-ping, LIU Hong-wu. A dynamical study of the role of surface heating on the Tibetan Plateau vortices [J]. J Trop Meteorol, 2006, 22(6): 632-637 (in Chinese).

[12] GAO Shou-ting, PING Fan. Laboratory studies of a stratified rotating flow past an isolated obstacle [J]. Chin Phys Lett, 2003, 20(7): 1 094-1 097 (in Chinese).

[13] YU Shu-hua, XIAO Yu-hua, GAO Wen-liang. Gold air influence on the Tibetan Plateau vortex moving out of the plateau [J]. J Appl Meteorol Sci, 2007, 18 (6): 737-747 (in Chinese).

[14] YU Shu-hua, GAO Wen-liang, XIAO Yu-hua. Analysis for the influence of cold air mass on two cases of plateau vortex moving out of the Tibetan Plateau [J]. Plateau Meteorol, 2008, 27(1): 96-103 (in Chinese).

[15] HE Guang-bi, GAO Wen-liang, TU Ni-ni. The dynamic diagnosis on eastwards moving characteristics and developing mechanism of two Tibetan Plateau vortex processes [J]. Acta Meteorol Sinica, 2009, 67 (4): 599-612 (in Chinese).

[16] HE Guang-bi, GAO Wen-liang, TU Ni-ni. The observation analysis of shear line and low vortex over the Tibetan Plateau in summer from 2000 to 2007 [J]. Plateau Meteorol, 2009, 28(3): 549-555 (in Chinese).

[17] LIU Xiao-ran, LI Guo-ping. Nonlinear singular inertial gravitational wave forced by diabatic heating and its association with the Tibetan Plateau vortex [J]. Plateau Meteorol, 2007, 26(2): 225-231 (in Chinese).

[18] CHEN Gong, LI Guo-ping. Characteristics of the tangential flow field of the Tibetan Plateau vortices and associ-

ated waves [J]. Acta Meteorol Sinica, 2011, 69 (6): 956-963 (in Chinese).
[19] SONG Wen-wen, LI Guo-ping, TANG Qian-kui. Numerical simulation of the effect of heating and water vapor on two cases of plateau vortex [J]. Chin J Atmos Sci, 2012, 36 (1): 117-129 (in Chinese).
[20] MADDEN R A, JULIAN P R. Detection of a 40-50 day oscillation in the zonal wind in the tropical Pacific [J]. J Atmos Sci, 1971, 28: 702-708.
[21] MADDEN R A, JULIAN P R. Description of globe scale circulation cells in the tropics with 40-50 day period [J]. J Atmos Sci, 1972, 29: 1 109-1 123.
[22] KRISHNAMURTI TN, GADGIL S. On the structure of the 30 to 50 day mode over the globe during FGGE [J]. Tellus, 1985, 45: 336-360.
[23] YASUNARI T. A quasistationary appearance of 30-40 day period in the fluctuations during the summer monsoon over India [J]. J Meteorol Soc Japan, 1980, 58: 225-229.
[24] ZHU Qian-gen. A review of studies on East Asia winter monsoon in China [J]. Meteorol Mon, 1990, 16(1): 3-10 (in Chinese).
[25] MIAO Jin-ha, LIU Jia-ming. Low frequency oscillation (30-60 day) of summer monsoon rainfall over East Asia [J]. Chin J Atmos Sci, 1991, 15(5): 65-71 (in Chinese).
[26] JIN Zu-hui, SUN Shu-qing. The characteristics of low frequency oscillations in winter monsoon over the eastern Asia [J]. Chin J Atmos Sci, 1996, 20 (1): 101-111 (in Chinese).
[27] LI Chong-yin, WU Jing-bo. On the onset of the South China Sea summer monsoon in 1998 [J]. Adv Atmos Sci, 2000, 17(2): 193-204.
[28] JU Jian-Hua, SUN Dan, LU Jun-Mei. The Influence of East Asian monsoon stream on the large-scale precipitation course in eastern China [J]. Chin J Atmos Sci, 2007, 31(6): 1 129-1 139 (in Chinese).
[29] JU Jian-hua, ZHAO Er-xu. Impacts of the low frequency oscillation in East Asian summer monsoon on the drought and flooding in the middle and lower valley of the Yangtze River [J]. J Trop Meteorol, 2005, 21(2): 163-171 (in Chinese).
[30] CHEN Li-zhen, ZHANG Xian-gong, CHEN Long-xun. A study of the difference of low-frequency oscillation between the typical flood/drought years in Changjiang Valley [J]. J Appl Meteorol, 1994, 4 (5): 483-488 (in Chinese).
[31] LU Er, DING Yi-hui. Low frequency oscillation in East Asia during the 1991 excessively heavy river basin [J]. Acta Meteorol Sinica, 1996, 54(6): 730-736 (in Chinese).
[32] HUANG Jing, ZHU Qian-gen. The characters of low-frequency circulation around the globe and its relationship with the flood/drought in the Changjiang River Valley [J]. J Trop Meteorol, 1997, 13(2): 146-157 (in Chinese).
[33] CHEN Long-xun, ZHU Cong-wen, WANG Wen, et al. Analysis of the characteristics of 30-60 day Low-frequency oscillation over Asia during 1998 SCSMEX [J]. Adv Atmos Sci, 2001, 18(4): 623-638.
[34] XU Guo-qiang, ZHU Qian-gen, BAI Hu-zhi. Rainfall features of the Tibetan Plateau and LFO influence on low frequency precipitation in the Yangtze River basin [J]. Sci Meteorol Sinica, 2003, 23(3): 282-291 (in Chinese).
[35] ZHOU Bing, HE Jin-hai, XU Hai-ming. LFO characteristics of meteorological elements over Tibetan Plateau and the relations with regional summer rainfall [J]. J Nanjing Inst Meteorol, 2003, 23(1): 93-100 (in Chinese).
[36] LU Jun-mei, JU Jian-hua, REN Ju-zhang, et al. The influence of the Madden-Julian oscillation activity anomalies on Yunnan's extreme drought of 2009-2010 [J]. Sci China: Ear Sci, 2012, 55 (1): 98-112 (in Chinese).
[37] HE Yi-hua, LI Cai-yuan, JIN Qi, et al. Relationship between the low frequency oscillation of TBB in summer of Qinghai Xizang Plateau and drought/ flood in central China [J]. Plateau Meteorol, 2006, 25(4): 658-664 (in Chinese).
[38] LI Chong-yin, ZHOU Ya-ping. Relationship between intraseasonal oscillation in the tropical atmosphere and ENSO [J]. Chin J Geophy, 1994, 37(1): 17-26 (in Chinese).
[39] LI Chong-yin, LIAO Qing-hai. The exciting mechanism of tropical intraseasonal oscillation to El Niño event [J]. J Trop Meteorol, 1998, 4(2): 113-121.
[40] LONG Zhen-xia, LI Chong-yin. Interannual Variability of 30-60 day low-frequency kinetic energy in the lower tropical atmosphere [J]. Chin J Atmos Sci, 2001, 25(6): 798-808 (in Chinese).
[41] QIU Ming-yu, LU Wei-song, TAO Li. Frequency modulation effect of ENSO events on atmospheric low-frequency oscillations in the extra-tropical latitudes [J]. J Nanjing Inst Meteorol, 2004, 27(3): 365-373.
[42] QIU Ming-yu, LU wei-song, CHEN Hui-lin, et al. Numerical experiments of effect of SSTA over the Indian Ocean on atmospheric low-frequency oscillation in the extratropical latitude [J]. J Trop Meteorol, 2007, 13(1): 73-76.
[43] SUN Guo-wu, CHEN Bao-de. Oscillation characteristics and meridional propagation of atmospheric low frequency waves over the Qinghai-Xizang Plateau [J]. Chin J Atmos Sci, 1988, 12(3): 250-256 (in Chinese).
[44] XIE An, YE Qian, CHEN Long-xun. The atmospheric oscillations over the Tibetan Plateau and surrounding areas as revealed [J]. Acta Meteorol Sinica, 1989, 47 (3): 272-278 (in Chinese).
[45] LI Yue-qing. The low-frequency oscillation over the Qinghai-Xizang plateau and the activities of the south Asia high during the summer half year in 1981 and 1982 [J]. Platcau Meteorol, 1996, 15(3): 276-281 (in Chinese).
[46] GONG Yuan-fa, XU Mei-ling, HE Jin-hai, et al. On the relationship between the eastern Tibet Plateau rainfall and subtropical high shift in summer [J]. Acta Meteorol Sinica, 2006, 649 (1): 90-99 (in Chinese).
[47] PENG Yu-ping, HE Jin-hai, CHEN Long-xun, et al. A study on the characteristics and effect of the low-frequency oscillation of the atmospheric heat source over the eastern Tibetan Plateau [J]. J Tropical Meteorol, 2014, 20 (1): 17-25.
[48] ZHANG Ji-jia SUN Guo-wu, CHEN Bao-de. Research on atmospheric low frequency change [M]. Beijing: Science Press, 1991: 60-67 (in Chinese).
[49] SUN Guo-wu, CHEN Bao-de. Characteristics of the Lows Flocking with Tibet atmospheric low-frequency oscillation over the Qinghai-Xizang (Tibet) Plateau [J]. Chin J Atmos Sci, 1994, 18(1): 113-121 (in Chinese).
[50] ZHANG Peng-fei, LI Guo-ping, FU Xiou-hua, et al. Clustering of Tibetan Plateau vortices by 10-30-day intraseasonal oscillation [J]. Mon Wea Rev, 2014, 142 (1): 290-300.

[51] PAN Jing, LI Chong-yin, SONG Jie. The modulation of Madden—Julian oscillation on typhoons in the northwestern Pacific Ocean [J]. Chin J Atmos Sci, 2010, 34(6): 1 059-1 070 (in Chinese).
[52] LI Chong-yin, PAN Jing, TIAN Hua, et al. Typhoon activities over the western north Pacific and atmospheric intraseasonal oscillation [J]. Meteorol Mon, 2012, 38(1): 1-16 (in Chinese).
[53] WHEELER M, HENDON H. An all-season real-rime multivariate MJO index: Development of an index for monitoring and Prediction [J]. Mon Wea Rev, 132: 1 917-1 932.
[54] QIAN Zhen-an, SHAN Fu-min, LU Jun-ning, et al. A statistic study of the summer vortex over Tibetan Plateau in 1979 and climate favoring the vortex [C]// Papers on the Tibetan Plateau Meteorological Experiment (Part Two), Beijing: Science Press, 1984: 182-194 (in Chinese).

Citation: ZHAO Fu-hu, LI Guo-ping, HUANG Chu-hui, et al. Modulation of Madden-Julian oscillation on Tibetan Plateau vortex [J]. J Trop Meteorol, 2016, 22(1): 30-41.